Radiation-pressure-driven vibrational modes in ultrahigh-Q silica microspheres

R. Ma,[1,2] A. Schliesser,[1] P. Del'Haye,[1] A. Dabirian,[1,3] G. Anetsberger,[1] and T. J. Kippenberg[1,*]

[1]*Max-Planck-Institut für Quantenoptik, Hans-Kopfermann-Strasse 1, 85748 Garching, Germany*
[2]*Present address, Technische Universität Hamburg-Harburg, 21073 Hamburg, Germany*
[3]*Present address, École Polytechnique Fédérale de Lausanne (EPFL), CH-1015 Lausanne, Switzerland*
[*]*Corresponding author: tjk@mpq.mpg.de*

Received February 20, 2007; revised June 1, 2007; accepted June 4, 2007;
posted June 18, 2007 (Doc. ID 80014); published July 24, 2007

Quantitative measurements of the vibrational eigenmodes in ultrahigh-Q silica microspheres are reported. The modes are excited via radiation-pressure-induced dynamical backaction of light confined in the optical whispering-gallery modes of the microspheres (i.e., via the parametric oscillation instability). Two families of modes are studied and their frequency dependence on sphere size investigated. The measured frequencies are in good agreement both with Lamb's theory and numerical finite-element simulation and are found to be proportional to the sphere's inverse diameter. In addition, the quality factors of the vibrational modes are studied. © 2007 Optical Society of America

OCIS codes: 190.4410, 270.3100, 300.0300.

Silica microcavities [1] such as microspheres or microtoroids [2] possess ultrahigh-Q optical whispering gallery modes (WGMs) while simultaneously exhibiting mechanical modes that lie typically in the radio frequency range. Owing to the resonant buildup of light within these cavities the effect of radiation pressure is enhanced, leading to mutual coupling between the mechanical and optical modes, as first predicted by Braginsky in the context of the Laser Interferometer Gravitational Wave Observatory (LIGO) [3]. When entering the regime where the photon lifetime is comparable with the mechanical oscillation period and the cavity is pumped with a laser whose frequency slightly exceeds the WGM resonance (i.e., blue-detuned excitation), this mutual coupling gives rise to a parametric oscillation instability [3] that is characterized by regenerative mechanical oscillation of the mechanical eigenmodes. This phenomenon was first reported in toroid microcavities [4–6]. On the other hand, red-detuned laser excitation can induce cooling of the mechanical modes [7–9]. In this Letter, the parametric oscillation instability in ultrahigh-Q silica microspheres is observed and the mechanical resonant frequencies and mode patterns are studied. In contrast to earlier studies of acoustic modes of nanospheres [10] using Raman or Brillouin scattering from ensembles, the present method allows measurement of the mechanical modes of single microspheres in a larger-diameter regime (35–110 μm in our case). Furthermore, the mechanical Q factors are determined.

Silica microspheres with ultrahigh optical Q ($Q > 10^8$) are fabricated by melting the tip of a single-mode optical fiber with a CO_2 laser ($\lambda = 10.6$ μm) and are held by a thin fiber stem (see Fig. 1 inset). The WGMs are excited with high ideality [11] by evanescent coupling via a tapered optical fiber using a 1550 nm tunable external cavity diode laser as pump source. Owing to the high finesse (exceeding 10^5), the large optical energy stored in the microcavity exerts a force on the cavity sidewalls that is due to radiation pressure. This force can give rise to regeneratively driven mechanical oscillations if the photon lifetime is comparable with the inverse acoustic resonance frequency [4,5]. In essence, the radial force exerted by radiation pressure takes the cavity out of resonance by deformation of the cavity wall, which subsequently causes a reduction in the radiation pressure force. The whole process resumes upon the restoration of the original shape of the cavity, leading

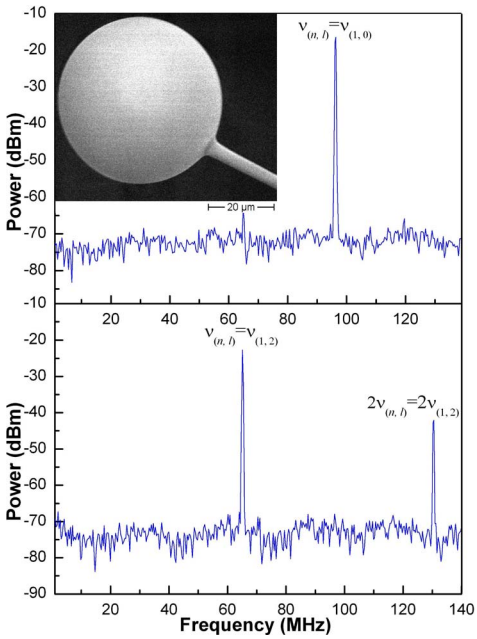

Fig. 1. (Color online) Radio-frequency spectrum of the photocurrent induced by the transmission of the fiber taper when coupled to a silica microsphere with a diameter of 49 μm. Two families of spheroidal mechanical modes could be driven regeneratively. Specifically, the modes are identified as $\nu_{(1,2)}$ (a quadrupole mode) and $\nu_{(1,0)}$ (a radial breathing mode). The launched power in this experiment was 600 μW and was sufficient to exceed the threshold for parametric oscillation instability. The inset shows the scanning electron microscope image of the microsphere.

0146-9592/07/152200-3/$15.00

to a periodic motion of the cavity. In this way, modes with radial deformation can be excited that modify the effective round-trip length of the optical WGM and consequently affect the magnitude of the radiation force. In the present experiments the threshold for the parametric instability was typically near 100 μW. The driven mechanical oscillation causes the appearance of motional sidebands (and their harmonics) with respect to the laser's frequency. With an electronic spectrum analyzer, the beat between the sidebands and the laser line can be readily observed in the photocurrent of a detector recording the power of the transmitted light. Figure 1 shows a typical photocurrent spectrum that clearly shows signatures of the regenerative mechanical oscillation of two different mechanical eigenmodes of the same sphere under different taper coupling conditions. Changing the taper loading (and hence the optical Q) causes the value of the oscillation threshold of the low- and the high-frequency mechanical modes to cross, thereby causing a switching from the low- to a high-frequency mode as coupling strength increases and the optical linewidth decreases, in agreement with the theoretical predictions [5]. To identify the mode families, the vibrational frequencies of the two observed mechanical frequencies were recorded as a function of size. While observable in principle, light-induced modifications of the mechanical modes' dynamical properties [9], in particular shifts in the mechanical resonance frequency, are considered to be small (relative frequency shift typically $<0.1\%$) and are neglected in this Letter. The result of this study is shown in Fig. 2. As is evident, the spheres' mechanical frequencies are inversely proportional to the spheres' diameter.

Next, the observed modes were identified by numerical studies. Since the fabricated silica microspheres exhibited a diameter ratio of the stem holding the sphere and the sphere itself of the order of 0.1, the sphere can be considered almost free; hence it is a judicious choice to adopt the stress-free boundary condition. Studies on the nature of the fundamental modes of vibration for small elastic spheres with free-surface boundary conditions are well known. The first well-established theory was formulated by Lamb, with two types of modes predicted, the spheroidal and torsional modes [12]. The equation describing the wave propagation in a homogeneous elastic body with free surface can be written as [13]

$$\rho\ddot{\mathbf{u}} = (\lambda + 2\mu)\,\nabla(\nabla\cdot\mathbf{u}) - \mu\,\nabla\times(\nabla\times\mathbf{u}), \tag{1}$$

where $\mathbf{u}$ is the displacement vector, ρ is the mass density, and λ and μ are Lamé constants. Here $\lambda \equiv \sigma E/[(1+\sigma)(1-2\sigma)]$, and $\mu \equiv E/[2(1+\sigma)]$, with E denoting the Young's modulus and σ the Poisson ratio of the material. Equation (1) can be solved by introducing a scalar potential ϕ_0 and two vector potentials $\Phi_1=(r\phi_1,0,0)$ and $\Phi_2=(r\phi_2,0,0)$ with $\mathbf{u}=\nabla\phi_0+\nabla\times\Phi_1+\nabla\times\nabla\times\Phi_2$. Then the general solutions of the equations resulting from Eq. (1) are written as

$$\phi_k(\mathbf{r},t) = \sum_{l,m} A_k^{(l,m)} j_l\left(\frac{2\pi\nu_{n,l,m}r}{V_k}\right) Y_l^m(\theta,\psi)e^{-2\pi i\nu_{n,l,m}t}, \tag{2}$$

where $k=0$, 1, 2, and j_l is the spherical Bessel function, Y_l^m is the spherical harmonic function, V_0 is the longitudinal sound velocity, and $V_1=V_2$ are the transverse sound velocities. An angular momentum mode number l ($l=0,1,2,\ldots$), an azimuthal mode number m ($-l\leqslant m\leqslant l$), and a radial mode number n ($n=1,2,\ldots$) are used to characterize the acoustic modes, where $n=1$ corresponds to the surface mode, $n\geqslant 2$ to inner modes, and $\nu_{n,l,m}$ denotes the frequency of the vibration characterized by the mode numbers (n,l,m). It is noteworthy that a spheroidal mode with angular momentum l is $(2l+1)$-fold degenerate; hence in Fig. 1 we use (n,l) instead of (n,l,m) to denote the eigenfrequencies.

Two classes of modes are derived when applying the free boundary condition [13]. One of them is the torsional vibration, which induces only shear stress without volume change, and no radial displacement takes place in these modes. These modes could not be excited by using radiation pressure in the present experiments, because the optical effective pathlength remains unchanged during mechanical motion. In contrast, the class of mode in which volume change is present is referred to as spheroidal. According to Lamb's theory the $l=0$ spheroidal mode eigenvalue equation is written as

$$\frac{\tan(hR)}{hR} - \frac{1}{1-\frac{1}{4}(k^2/h^2)h^2R^2} = 0, \tag{3}$$

where $k=2\pi\nu/V_1$, $h=2\pi\nu/V_0$, R is the radius of the sphere, $V_0=\sqrt{(\lambda+2\mu)/\rho}$, and $V_1=V_2=\sqrt{\mu/\rho}$. Other ei-

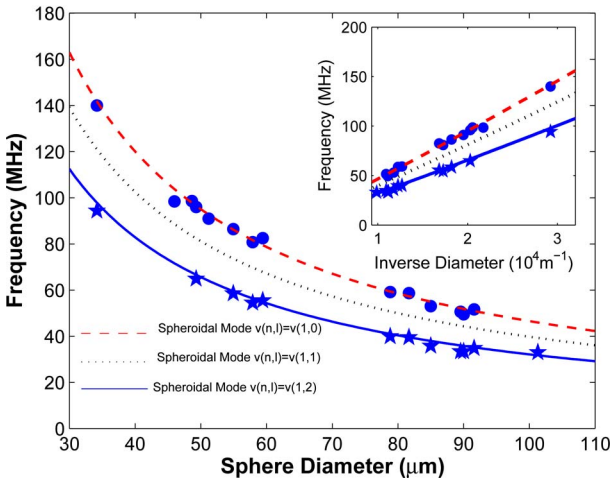

Fig. 2. (Color online) Experimentally measured frequencies of the spheroidal modes, with stars denoting the $\nu_{(1,2)}$ mode and dots denoting the $\nu_{(1,0)}$ mode. Numerically calculated eigenfrequencies of these modes are shown as the solid line ($\nu_{(1,2)}$) and the dashed line ($\nu_{(1,0)}$). The spheroidal mode $\nu_{(1,1)}$ has a frequency that lies between $\nu_{(1,2)}$ and $\nu_{(1,0)}$ and is not experimentally observed (dotted line). The inset shows the relationship between the frequencies of the eigenmodes and the inverse diameter of the silica microspheres.

genvalue equations for torsional modes and $l>0$ spheroidal modes are contained in Ref. [12]. Next, the resonant frequencies of the first three lowest lying frequencies (i.e., $n=1, l=0,1,2$) were numerically calculated as a function of sphere size (compare Fig. 2, solid curves). The eigenvalues versus the inverse of the diameters are shown in the inset. As is seen from Fig. 2, the measured data fit very well to the theoretical prediction based on the $\nu_{(1,0)}$ (radial breathing) and $\nu_{(1,2)}$ (quadrupole) mode and reveal that the eigenfrequencies of the microspheres have a linear dependence on the inverse microsphere diameter. We note that the sphere's eccentricity can partially lift the $(2l+1)$-fold degeneracy in the mode number m of the $\nu_{(1,2)}$ mode [14]. Analysis of the splitting in the degeneracy-lifted azimuthal optical WGMs (which exhibited splitting near ~100 MHz) allowed us to infer the typical level of eccentricity ($\sim 10^{-3}$). Note that the eccentricity, along with the fact that the stem perturbs the mechanical mode, leads to an observable mode splitting in the $l=2$ vibrational mode in the range of typically 10–100 kHz.

It is worth pointing out that the $l=1$ spheroidal mode has an eigenfrequency lying between the $l=0$ and $l=2$ spheroidal modes (Fig. 2); However, it results in too small a path length change around the optical WGM trajectory. Thus the mutual coupling of the optical and the $l=1$ mechanical mode could not be observed in the experiment.

To gain a more complete understanding of the mechanical modes, the numerical studies were complemented with finite-element simulations of the stress and strain fields. Using axial symmetric finite-element modeling, the mode families $\nu_{(1,0)}$ and $\nu_{(1,2)}$ were calculated, and excellent agreement was found with the numerical solution of the preceding section. Figure 3 depicts the strain and von Mises stress, as obtained from finite-element simulations of two spheroidal modes with the lowest frequencies. The strain is greatly exaggerated for clarity.

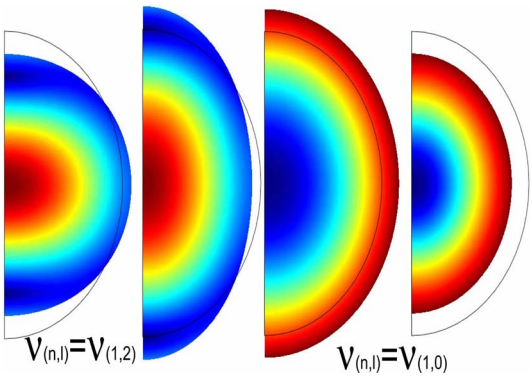

Fig. 3. (Color online) Finite-element modeling of three spheroidal modes, $\nu_{(1,2)}$ (left), and $\nu_{(1,0)}$ (right) of a silica microsphere with its von Mises stress (color coded), and strain (greatly exaggerated for clarity).

To determine the mechanical dissipation of the vibrational modes, the mechanical quality factor of the sphere modes was measured in the subthreshold regime (in a purged nitrogen environment). For this measurement the laser power was adjusted to a level far below the threshold of the mechanical oscillation. In addition, the mechanical Q factor was measured for both blue detuning (i.e., where the radiation pressure decreases the mechanical dissipation, causing mechanical amplification) and red detuning (where the radiation pressure causes the mechanical damping to be increased, leading to cooling). At suitably low power (and thus with marginal radiation-pressure-induced amplification or cooling of mechanical modes), both values coincided closely and yielded Q values of up to ~10,000 for the radial breathing mode. In vacuum, this factor improved to values of ~20,000.

We thank D. Grundler and P. Berberich in the Physics Department of the Technical University of Munich for providing access to the scanning electron microscope. This work was funded by a Max Planck Independent Junior Research Group grant, a Marie Curie International Reintegration Grant (CMIRG-CT-2005-031141), a Marie Curie Excellence Grant (MEXT-CT-2006-042842) and the Deutsche Forschungsgemeinschaft Nanoscience Initiative Munich.

References

1. K. J. Vahala, Nature **424**, 839 (2003).
2. D. K. Armani, T. J. Kippenberg, S. M. Spillane, and K. J. Vahala, Nature **421**, 925 (2003).
3. V. B. Braginsky, S. E. Strigin, and S. P. Vyatchanin, Phys. Lett. A **287**, 331 (2001).
4. H. Rokhsari, T. J. Kippenberg, T. Carmon, and K. J. Vahala, Opt. Express **13**, 5293 (2005).
5. T. J. Kippenberg, H. Rokhsari, T. Carmon, A. Scherer, and K. J. Vahala, Phys. Rev. Lett. **95**, 033901 (2005).
6. T. Carmon, H. Rokhsari, L. Yang, T. J. Kippenberg, and K. J. Vahala, Phys. Rev. Lett. **94**, 223902 (2005).
7. S. Gigan, H. R. Bohm, M. Paternostro, F. Blaser, G. Langer, J. B. Hertzberg, K. C. Schwab, D. Bauerle, M. Aspelmeyer, and A. Zeilinger, Nature **444**, 67 (2006).
8. O. Arcizet, P. F. Cohadon, T. Briant, M. Pinard, and A. Heidmann, Nature **444**, 71 (2006).
9. A. Schliesser, P. Del'Haye, N. Nooshi, K. J. Vahala, and T. J. Kippenberg, Phys. Rev. Lett. **97**, 243905 (2006).
10. M. H. Kuok, H. S. Lim, S. C. Ng, N. N. Liu, and Z. K. Wang, Phys. Rev. Lett. **90**, 255502 (2003).
11. S. M. Spillane, T. J. Kippenberg, O. J. Painter, and K. J. Vahala, Phys. Rev. Lett. **91**, 043902 (2003).
12. H. Lamb, Proc. London Math. Soc. **13**, 189 (1882).
13. N. Nishiguchi and T. Sakuma, Solid State Commun. **38**, 1073 (1981).
14. A. Tamura, K. Higeta, and T. Ichinokawa, J. Phys. C **15**, 4975 (1982).